



# Characterization of Grinding-Induced Subvisible Particles and Free Radicals in a Freeze-Dried Monoclonal Antibody Formulation

Zhen-Yi Jing<sup>1,2</sup> · Guo-Li Huo<sup>1,2</sup> · Min-Fei Sun<sup>1,2</sup> · Bin-Bin Shen<sup>1,2</sup> · Wei-Jie Fang<sup>1,2</sup>

Received: 2 December 2021 / Accepted: 14 January 2022 / Published online: 26 January 2022  
© The Author(s), under exclusive licence to Springer Science+Business Media, LLC, part of Springer Nature 2022

## ABSTRACT

**Purposes** The primary objectives of this study were to investigate the degradation mechanisms of freeze-dried monoclonal antibody (mAb) formulations under mechanical grinding, assess the sensitivity and suitability of various particle analysis techniques, analyze the structure of the collected subvisible particles (SbVPs), and analyze the antioxidant mechanism of methionine (Met) under degradation process to gain a thorough understanding of the phenomenon.

**Methods** The freeze-dried mAb-X formulations underwent grinding, and the resultant SbVPs were characterized through visual inspection, flow imaging microscopy, dynamic light scattering, ultraviolet–visible spectroscopy, and size-exclusion high-performance liquid chromatography. We further evaluated the effect of different temperatures and the free radical scavenger Met on SbVP formation. The produced free radicals were detected using electron paramagnetic resonance, and Met S-oxide formation was detected using liquid chromatography–mass spectrometry. In addition, we analyzed the obtained SbVPs using capillary electrophoresis sodium dodecyl sulfate and Fourier transform infrared spectroscopy.

**Results** Grinding leads to SbVP formation under high temperature and free radical formation. Free radicals produced during grinding require the participation of a macromolecule. Met could then bind to the produced free radicals, thus partially protecting mAb-X from degradation while itself undergoing oxidation to form Met(O). Sensitivity differences between different particle analysis techniques were evaluated,

and the obtained SbVPs showed significant changes in secondary structure and the formation of covalent aggregates and fragments.

**Conclusions** Met plays the role of an antioxidant in protecting macromolecules by quenching the free radicals produced during grinding. To thoroughly characterize SbVPs, multiple and orthogonal particle analysis techniques should be used, and if necessary, SbVPs should be processed by enrichment to accurately analyze primary and high order structures.

**KEY WORDS** aggregation · flow imaging microscopy · free radical · grinding · Met(O) · monoclonal antibody · protein subvisible particles

## ABBREVIATIONS

CD	circular dichroism
CE-SDS	capillary electrophoresis sodium dodecyl sulfate
DLS	dynamic light scattering
EPR	electron paramagnetic resonance
FIM	flow imaging microscopy
FT-IR	Fourier transform infrared spectroscopy
LC-MS	liquid chromatography–mass spectrometry
mAb	monoclonal antibody
Met	methionine
Met(O)	methionine S-oxide
OD	optical density
PES	polyethylstyrene
SbVP	subvisible particle
SE-	size-exclusion high-performance liquid
HPLC	chromatography
TIC	total ion chromatogram
UV-Vis	ultraviolet–visible spectroscopy

✉ Wei-Jie Fang  
wjfang@zju.edu.cn

<sup>1</sup> Institute of Drug Metabolism and Pharmaceutical Analysis, College of Pharmaceutical Sciences, Zhejiang University, Hangzhou 310058, China

<sup>2</sup> Hangzhou Institute of Innovative Medicine, Zhejiang University, Hangzhou 310016, China

## INTRODUCTION

Biopharmaceuticals, or protein-based drugs, are fast-growing therapeutic modalities for treating human diseases. Among them, monoclonal antibodies (mAbs) have made significant contributions in the fields of infection, cancer, and autoimmune illnesses (1). However, due to their complex and unstable structure, controlling and analyzing their stability have become increasingly challenging. Among them, the generation of aggregates and subvisible particles (SbVPs) is increasingly emphasized. They are the most common product-related impurities, which can cause immunogenicity or loss of biological activity (2). Temperature, interface effects, light, and mechanical stress can all induce their production (3). Presently, more individuals are realizing that in the supply, use, and process of biopharmaceutical production, more emphasis should be placed on research for the development and control of aggregates and SbVPs to ensure the quality of protein medications.

Physical degradation will produce various aggregates and SbVPs with sizes ranging from nanometers, submicrometers to micrometers. One main problem in the characterization of SbVPs is that there is no analytical approach that can cover the entire size range of aggregates that may occur. Several studies have reported that different analytical methods, such as size-exclusion high-performance liquid chromatography (SE-HPLC), dynamic light scattering (DLS), light obscuration, and visible particle analysis, are recommended when studying aggregates produced by mAbs to cover the size range from a few nanometers to 100  $\mu\text{m}$  to large visible molecules (4). After a comprehensive analysis, it can be determined whether larger protein aggregates are generated in the sample, thereby avoiding that. It is practically impossible to correctly estimate its true state of size and morphology using only one method (5).

Mechanical stress is one of the most underestimated sources of aggregation. During production or transportation, proteins may be subjected to high shear or mechanical stress through agitation, mixing, or dropping, as well as being exposed to various interfaces thereby producing large amounts of SbVPs (6,7). A series of studies induced stress, including mechanical stresses such as stirring (or shaking) and shipping, on protein formulations in the liquid state to investigate the characteristics of SbVPs formed (8–12). Freeze-dried mAb formulations often exhibit higher physicochemical stability during storage and transportation than that of liquid formulations, potentially extending the storage period and reducing aggregation. Most proteins are more stable at high temperatures in freeze-dried dosage forms. However, if they are mechanically stressed during the production and transportation, freeze-dried dosage forms may not withstand the physicochemical damage caused (13–15).

As reported in a previously published paper by our laboratory, a freeze-dried mAb formulation produced SbVPs under mechanical grinding stress, and the mechanism underlying it was investigated (16). This study investigated whether the same phenomenon is true for another mAb (mAb-X) formulation and aimed to provide more insights. Regarding the generation of aggregates, previous papers have used methods such as micro-flow imaging (MFI), DLS, and SE-HPLC to detect particles produced by gentle grinding for 30 s. However, in this study, we discovered that by extending the grinding time, the results of various particle analysis techniques show some differences. This study also detected the structure of the SbVPs produced by grinding after collection using methods such as Fourier transform infrared spectroscopy (FT-IR) and capillary electrophoresis sodium dodecyl sulfate (CE-SDS). Moreover, the antioxidant mechanism of methionine (Met) as a free radical scavenger was investigated using liquid chromatography–mass spectrometry (LC–MS).

## MATERIALS AND METHODS

### Materials

Freeze-dried mAb-X formulation was generously provided by Zhejiang Bioray Biopharmaceutical (Zhejiang, China). This formulation powder included 100 mg mAb-X, 0.5 mg polysorbate 80, 500 mg sucrose, 6.1 mg disodium hydrogen phosphate dodecahydrate, and 2.2 mg sodium dihydrogen phosphate dihydrate. Sucrose was purchased from Merck KGaA (Darmstadt, Germany) and polysorbate 80 was purchased from Nanjing Well Pharmaceutical (Nanjing, China). Isopropanol, sodium chloride, disodium hydrogen phosphate dodecahydrate, and sodium dihydrogen phosphate dihydrate were purchased from Sinopharm Chemical Reagent CO., Ltd. (Shanghai, China). 0.22  $\mu\text{m}$  polyethylstyrene (PES) membrane filters were purchased from Millipore (Burlington, MA, USA). Met was purchased from JTBaker (Lardner, Illinois, USA), trifluoroacetic acid was purchased from Sarn Chemical Technology (Shanghai, China), and acetonitrile was purchased from Sigma-Aldrich (St. Louis, MO, USA).

### Sample Preparation

mAb-X samples were obtained from Zhejiang Bioray Biopharmaceutical (Zhejiang, China). mAb-X was reconstituted with water as a control formulation or a solution of 20 mM Met as the test formulation; these were labeled as CONTROL and MET, respectively. Two corresponding placebo formulations (without mAb-X) were prepared, labeled as PLACEBO CONTROL (without Met) and PLACEBO MET (with Met).

Each formulation was finely filtered into a centrifuge tube using 0.22- $\mu\text{m}$  PES membrane filters and 1 mL was poured into 2-mL vials. After weighing, the samples were placed in a VirTis AdVantage freeze-dryer (Los Angeles, CA, USA) for 2 h, where it froze to  $-40^{\circ}\text{C}$  at a rate of  $0.5^{\circ}\text{C}/\text{min}$ . In the annealing step, the shelf temperature was increased to  $-20^{\circ}\text{C}$  within 30 min and maintained for 2 h. The pressure and temperature of the primary drying were 60 mTorr and  $-12^{\circ}\text{C}$ , respectively. The conditions were maintained for 25 h, and the shelf temperature was increased to  $30^{\circ}\text{C}$  at a rate of  $0.2^{\circ}\text{C}/\text{min}$  and maintained at  $30^{\circ}\text{C}$  for 4 h. The quality of the finished product was evaluated and compared with the solution before the freeze-drying process.

### Mechanical Stress Conditions

After freeze-drying, the CONTROL and MET formulation powder in the 2-mL vials was gently ground for 30 s using a 4-mm glass tube. Then, the unground particles and ground powder was dissolved in distilled water to form a 20-mg/mL protein solution for FIM, DLS, visual inspection, and SE-HPLC or 0.4-mg/mL protein solution for UV-Vis analysis. To confirm whether grinding would induce protein chemical degradation reactions (i.e., covalent aggregation and fragmentation), the mAb-X formulation powder was ground at room temperature with the same intensity for 30 min, and then visually inspected or subjected to with DLS and SE-HPLC. To assess the different sensitivities of FIM, DLS, and SE-HPLC in characterizing SbVPs, the mAb-X formulation powder was ground at the same intensity for 1 and 10 min at room temperature and then examined via visual inspection, FIM, DLS, UV-Vis, and SE-HPLC(16). To determine the structure of the SbVPs produced after grinding, the particles were enriched by centrifugation and washed several times before freeze-drying; this sample was labeled as PARTICLES.

### Visual Inspection

The samples were placed on the edge of the light-shielding plate, and, using the neck of the container, were held at a clear viewing distance (usually 25 cm), gently rotated to prevent bubble formation, and checked against a black and white background. During inspection, illuminance was set to 1000–1500 lx in the testing area. The total inspection time limit was 20 s. The samples were also assessed by measuring the optical density at 350 nm ( $\text{OD}_{350}$ ) using a Shimadzu UV-1800 Spectrophotometer (Suzhou, China).

### FIM Analysis

A FlowCam 8100 (Fluid Imaging Technologies, Yarmouth, ME, USA) equipped with an 80- $\mu\text{m}$  field, 1-mL syringe, and a 10-fold objective was used in this study. System suitability for

particle size was measured by analyzing 5- $\mu\text{m}$  NIST traceable standards (Thermo Fisher Scientific, Waltham, MA, USA). We analyzed a sample volume of 0.2 mL at a flow rate of 0.1 mL/min. The attached VisualSpreadsheet software was used to acquire and process data.

### DLS

We measured SbVP formation using a Malvern Zetasizer Nano ZS90 ZEN 3690 (Malvern Instruments Ltd., Worcestershire, UK) instrument. We added 200  $\mu\text{L}$  of the sample to the sample pool in the measuring tank of the instrument. The measurement mode was set as size, the temperature, balance time, and detection angle were  $25^{\circ}\text{C}$ , 120 s, and  $90^{\circ}$ , respectively. All data were scanned in triplicate and averaged. The differences in the particle size distribution of the samples were analyzed and compared in terms of average particle size, intensity, volume, and quantity as per the scanning results.

### UV-Vis Spectroscopy

A Shimadzu UV-1800 Spectrophotometer (Suzhou, China) was used to determine the concentration of mAb-X at 260–350 nm. We calculated the protein concentration separately by applying the Beer-Lambert equation: protein concentration (mg/mL) =  $(\text{OD}_{280} - \text{OD}_{350}) \times \text{dilution factor} / \text{extinction coefficient}$  (1.49).

### SE-HPLC with UV Analysis

SE-HPLC was performed using an Agilent 1200 series HPLC system (Agilent Technologies, Santa Clara, CA, USA) with UV detection at 280 nm, as previously described (16). Before analysis, samples were centrifuged for 10 min at 8000 rpm, and the peak area and percentage of the aggregates, monomer, and fragments were analyzed using the Agilent ChemStation software.

### Continuous-Wave Electron Paramagnetic Resonance

A Bruker A300 EPR spectrometer (Billerica, Maryland, USA) was used to analyze the 9.5-GHz X-band electron paramagnetic resonance (EPR) spectra of the ground and unground CONTROL formulation powders. Approximately 20 mg of each sample was measured in a 4-mm quartz EPR tube (Wilmad LabGlass, Vineland, NJ) located in the center of the microwave cavity. Typical EPR parameters used are as follows: power, 20.34 mW; microwave frequency, 9.859 GHz; central field, 3300 G; receiver gain,  $3.17 \times 10^4$ ; modulation amplitude, 2 G; modulation frequency, 100 kHz; conversion time, 40 ms; time constant, 81.92 ms with one X-Scan.

## FT-IR

Infrared spectra of mAb-X in freeze-dried formulations and concentrated particles were collected at room temperature using an FT/IR-4100 (JASCO, Japan). An appropriate amount of potassium bromide (approximately 500 mg) was taken and ground into a fine powder in an agate mortar; then, a small amount of formulation sample (approximately 1–2 mg of protein) was added, and grinding was continued. Subsequently, the fine powder was compressed into a transparent flake for testing. The final protein spectra were smoothed using a seven-point Savitsky–Golay function. The spectra were derived by second-order derivative, and the area was normalized between 1600 and 1670  $\text{cm}^{-1}$ .

## CE-SDS

To assess the formation of covalent aggregates and fragments after grinding for 30 min, we performed CE-SDS analyses in the nonreduced model using an Agilent 7100 high-performance capillary electrophoresis system, as previously described (16).

## LC-MS

The MET and PLACEBO MET samples before and after grinding for 30 min were evaluated by LC-MS using an Agilent 1290 series UPLC system interfaced with an Agilent 6460 Triple Quad mass spectrometer. Samples were diluted to 4 mg/mL mAb-X or equivalent with pure water, mixed thoroughly, and centrifuged at 13800 rpm for 5 min. The supernatant was then ultrafiltrated using a Millipore ultrafiltration tube (Amicon-Ultra-15, MWCO 10 kDa) at 4000 rpm for 2 h. Met oxidation was evaluated using an Elite Supresil ODS2 chromatographic column (4.6 × 250 mm, 5  $\mu\text{m}$ ). Mobile phase A included 0.1% trifluoroacetic acid aqueous solution, whereas mobile phase B included 0.1% trifluoroacetic acid in acetonitrile. A linear gradient of 5%–20% solvent B over 25 min was used. The injection volume was 5  $\mu\text{L}$ , the flow rate was 0.25 mL/min, the detection wavelength was 280 nm, the column temperature was 80°C, and the elution time was 20 min. We performed mass spectrometry using total ion chromatogram (TIC) full-ion scanning with scans ranging from 50 to 1000 amu.

## RESULTS

### Effect of the Freeze-Drying on SbVP Formation

The freeze-dried samples were reconstituted using the same amount of water lost during freeze-drying and analyzed using SE-HPLC, UV-Vis, FIM, and DLS; all results indicated no

significant change in the control and Met formulations before and after freeze-drying. This indicates that the freeze-drying process did not enhance SbVP production.

### Visual Inspection

The unground samples and the samples ground for 30 s were both clear after reconstitution. We observed no visible particles (>100  $\mu\text{m}$ ) (Fig. 4A). After grinding for 1 min, the optical density slightly increased; however, no visible particle was observed (Fig. 4A and B). After grinding for 30 min, a significant number of visible particles were detected (Fig. 4A and B).

### Detection of SbVPs after Grinding for 30 S

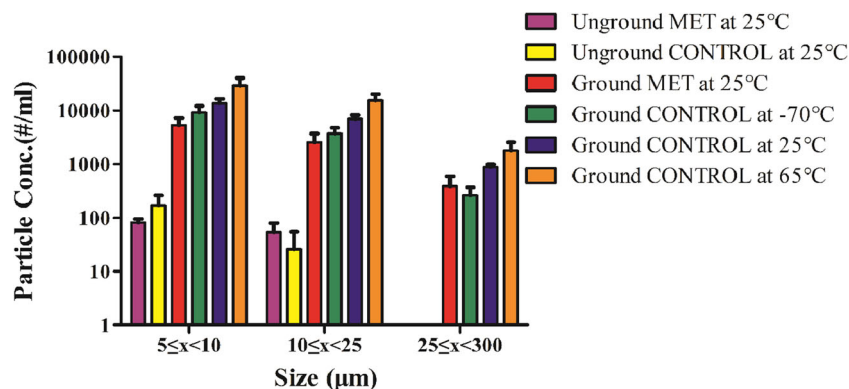
FIM results were used to investigate SbVP formation, as shown in Fig. 1. Without grinding, only a few insoluble SbVPs were formed, with an SbVP concentration above 5  $\mu\text{m}$  of 196 particles/mL. After gentle grinding at 25°C for 30 s, the SbVP concentration above 5  $\mu\text{m}$  was 21,558 particles/mL. SbVPs also exhibited consistent morphology (Fig. 2). Met, as a free radical scavenger, significantly reduced the number of SbVPs during grinding. The concentration of SbVPs above 5  $\mu\text{m}$  in the MET formulation was only 8235 particles/mL. The number of SbVPs formed was directly associated with grinding temperature. After grinding the mAb-X formulations at -70°C, 25°C, and 65°C, the numbers of SbVPs above 5  $\mu\text{m}$  were 13,220, 21,558, and 46,285 particles/mL, respectively (Fig. 1).

After comparing the changes in the number of SbVPs before and after grinding the protein-free PLACEBO CONTROL formulation at room temperature, the possibility that the grinding process itself would cause a significant difference in the number of SbVPs was excluded (data not shown).

DLS is a sensitive technique for characterizing a small number of SbVPs in a solution. For all formulations, the PDI (distribution coefficient) ranged from 0.08 to 0.7, indicating that all systems were with moderate dispersion and in the best applicable range of the algorithm. For the unground formulation, only one main peak (hydrodynamic diameter of approximately 35.7 nm) was obtained. After the sample was ground for 30 s, an extra peak >1  $\mu\text{m}$  appeared occasionally with a hydrodynamic diameter of approximately 4530 nm, but its percentage was extremely low (data not shown).

Currently, only EPR can detect free radicals directly (17). After grinding, the powder was evaluated using a continuous-wave 9.5 GHz X-band EPR (16). The ground powder exhibited an additional signal ( $g = 2.003$ ) in the EPR spectrum compared with the unground sample, indicating that a significant number of free radicals were produced during the process (Fig. 3A). The production of free radicals also correlated with grinding temperature, i.e., grinding at higher

**Fig. 1** Particle concentration and distribution of mAb-X formulations with or without Met for the un-ground samples and samples ground at different temperatures as measured using flow imaging microscopy.



temperatures caused more free radicals. The formed free radicals gradually disappeared over time (Fig. 3A).

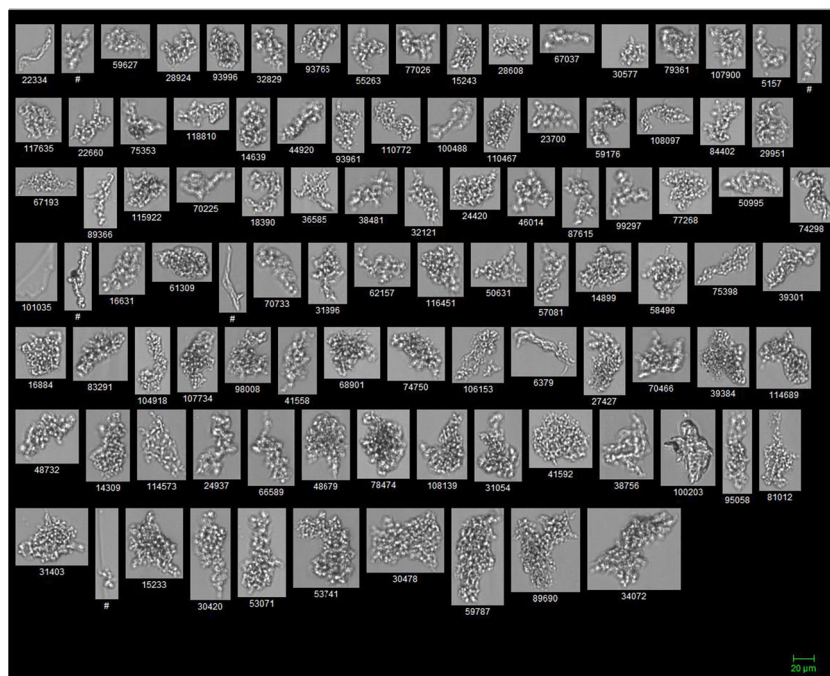
As shown in Fig. 3B, Met could effectively inhibit free radical formation, indicating that, in addition to the known mechanisms of thermally induced protein degradation, free radical formation is probably one of the underlying causes of protein SbVP formation when physical forces, such as grinding, are applied to the protein powder.

The two protein-free PLACEBO CONTROL and PLACEBO MET formulations exhibited no EPR signal under grinding (Fig. 3B), inferring that there could be two possible reasons, the first being the absence of free radical formation and the other being the easy quenching of free radicals formed by small molecules, which were subsequently analyzed using LC–MS to determine the exact mechanism.

### Physical Degradation of mAb-X after Grinding as Measured Using UV–Vis and SE-HPLC

We measured the physical degradation of mAb-X, such as the formation of soluble and insoluble aggregates after grinding, using UV–Vis spectroscopy. The UV–Vis spectroscopy revealed that the protein content of all formulations remained unaltered after grinding for 30 s. Similar to the UV–Vis results, no physical degradation of the samples after grinding was detected using SE-HPLC. Although the SbVPs detected using FIM significantly increased, the soluble and insoluble aggregates (i.e., loss of soluble protein) could not be detected by SE-HPLC. The purity and peak area of the mAb-X monomer did not significantly change after grinding (data not shown).

**Fig. 2** Representative images of SbVPs (>25 µm) as measured using flow imaging microscopy.



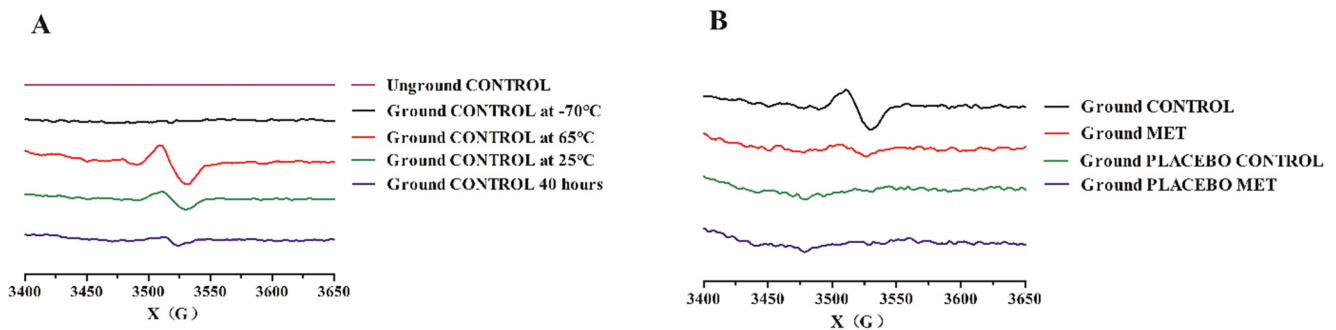


**Fig. 3** Electron paramagnetic resonance spectra of (A) the CONTROL formulations unground and ground at different temperatures and (B) protein formulation with or without proteins and Met ground at room temperature (25°C).

### Effect of Prolonged Grinding on the Quality of mAb-X

As shown in Fig. 4, visual inspection, FIM, DLS, SE-HPLC, and UV-Vis techniques were used to characterize the SbVPs formed. Furthermore, we discovered that with a slight increase in the grinding time, the number of SbVPs significantly increased in the FIM results (Fig. 4C). Meanwhile, a second peak around 3500 nm with an intensity percentage of 10% was observed in DLS (Fig. 4D), and the visual appearance was slightly less clear than the unground sample with no visible particles (Fig. 4A). Visual inspection results could all be matched to the turbidity ( $OD_{350}$ ) values (Fig. 4B). After increasing the grinding time to 10 min, visible particles appeared (Fig. 4A), SE-HPLC displayed a slight decrease in peak area (Fig. 4E), and UV-Vis analysis revealed a slight decrease in protein concentration (Fig. 4F). After 30 min of grinding at the same intensity, clarity was significantly reduced and visible particles were evident (Fig. 4A). Two additional peaks appeared in the DLS with hydrodynamic diameters of approximately 610 nm and 4950 nm (Fig. 4D). A significant decrease in the percentage of the main peak area was observed by SE-HPLC (Fig. 4E) and similarly, the protein concentration significantly decreased as determined by UV-Vis (Fig. 4F). The latter two time points, 10 min and 30 min, were not measured here using FIM because the SbVPs were overwhelming to be accurately measured.

### Characterization of the Grinding-Induced SbVPs after Collection

The SbVPs formed were recovered by centrifuging the ground samples for 30 min followed by freeze-drying. Simultaneously, the untreated mAb-X solution was boiled and freeze-dried, and then characterized using FT-IR. In the FT-IR spectra of boiled and collected particles, the peak intensity around  $1640\text{ cm}^{-1}$  was significantly reduced and an additional peak around  $1627\text{ cm}^{-1}$  was observed, indicating that the intramolecular  $\beta$ -sheet secondary structures at the native mAb-X became intermolecular  $\beta$ -sheet secondary structures during grinding, but this phenomenon could only

be measured when the SbVPs were enriched and collected, as shown in Fig. 5A. Some covalent aggregates and fragments appeared in the collected SbVPs measured using nonreduced CE-SDS (Fig. 5B), indicating that the chemical compositions of the particles were extremely complex, i.e., they consisted of covalent and noncovalent aggregates and fragments.

### Studies on the Protection Mechanism of Met Activity

Met oxidation can result in the generation of methionine S-sulfoxide (Met(O)) with molecular weight increase of 16 Da (18,19). The oxidation levels were calculated by dividing the TIC peak areas of the Met(O) by that of the original Met. As shown in Fig. 6, Met was oxidized to significant levels after grinding for 30 min in the control Met formulation. Low levels of oxidation of Met were observed in the placebo, indicating that Met was not easily oxidized under the action of grinding without mAb-X. Therefore, the presence of a macromolecule is a prerequisite for the formation of free radicals during grinding.

## DISCUSSION

Grinding is a mechanical stress that generates frictional interaction between the contact surfaces of the freeze-dried cake particles. It is not commonly used in the biopharmaceutical industry but has some applications, including inhalation administration of protein powders and the production process of some new manufacturing processes or dosage forms, such as electrospun fibers (20,21), dispersion of samples to make PLGA (22), freeze-dried vaccine formulations (23,24), including biopharmaceutical tablets, the mechanical stress of grinding also occurs during the preparation process, such as the granulation and the tableting process (25–28). Among them, electrostatic spinning (ES) is a novel and efficient continuous drying technology that can provide fast and gentle drying at room temperature. However, since the newly produced fiber does not have good processability, it needs to be ground. Grinding will also appear in the

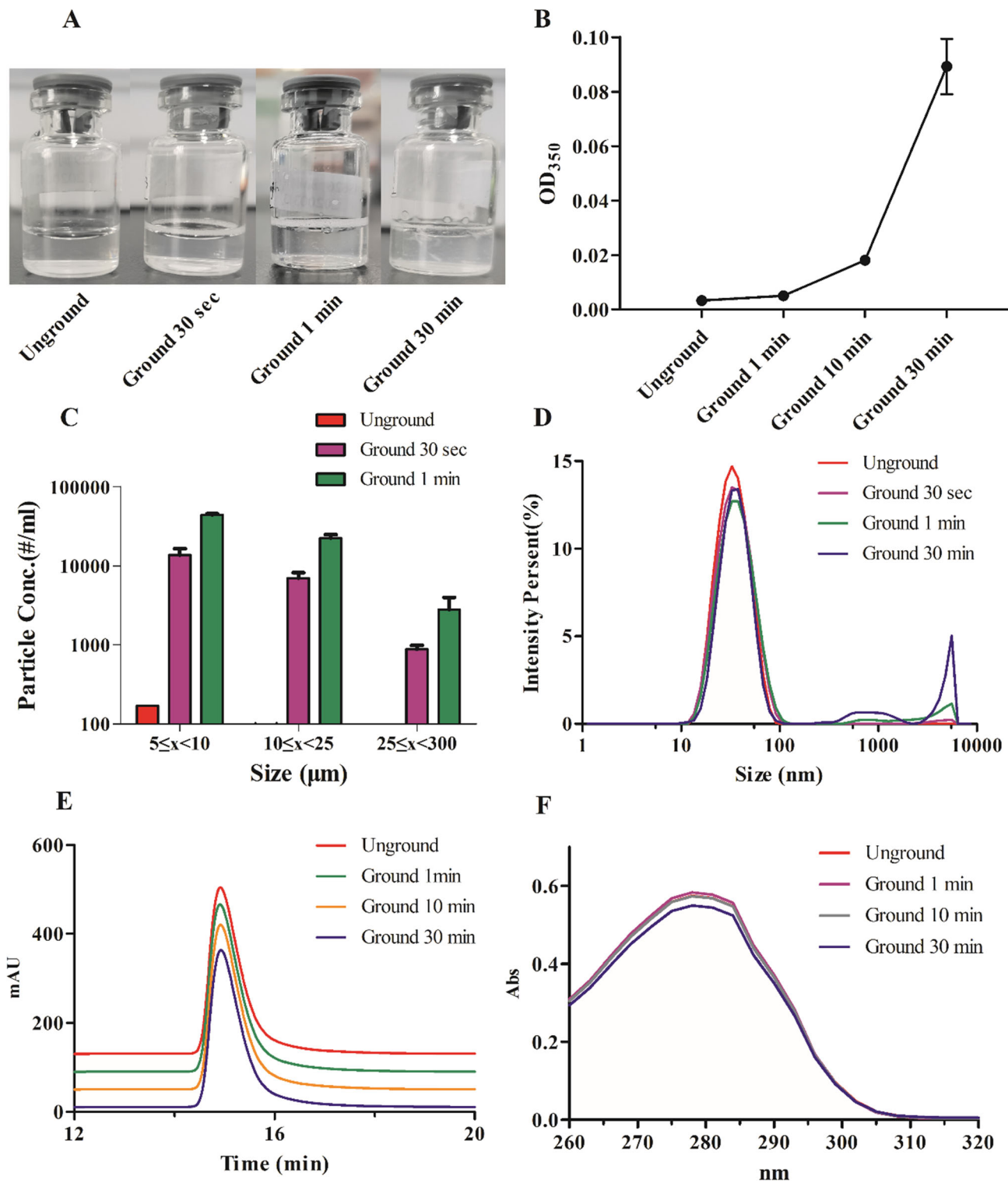


**Fig. 4** Effects of grinding time on the physical stability of mAb-X control formulation. (**A**) Results of visual inspection; (**B**) turbidity (OD<sub>350</sub>) analysis; (**C**) particle concentration and distribution measured using FIM; (**D**) light intensity particle distribution measured using DLS; (**E**) representative chromatograms measured using SE-HPLC; (**F**) representative absorption curves measured using UV-Vis.

early particle size reduction process and the later micro-encapsulation process when preparing PLGA, PLA and other dispersions by means of hot melt extrusion (HME)(22,29). Some researchers have also explored the

changes in the secondary structure of some non-pharmaceutical proteins during the grinding process, such as silk particles for targeted biomedical applications (30,31).

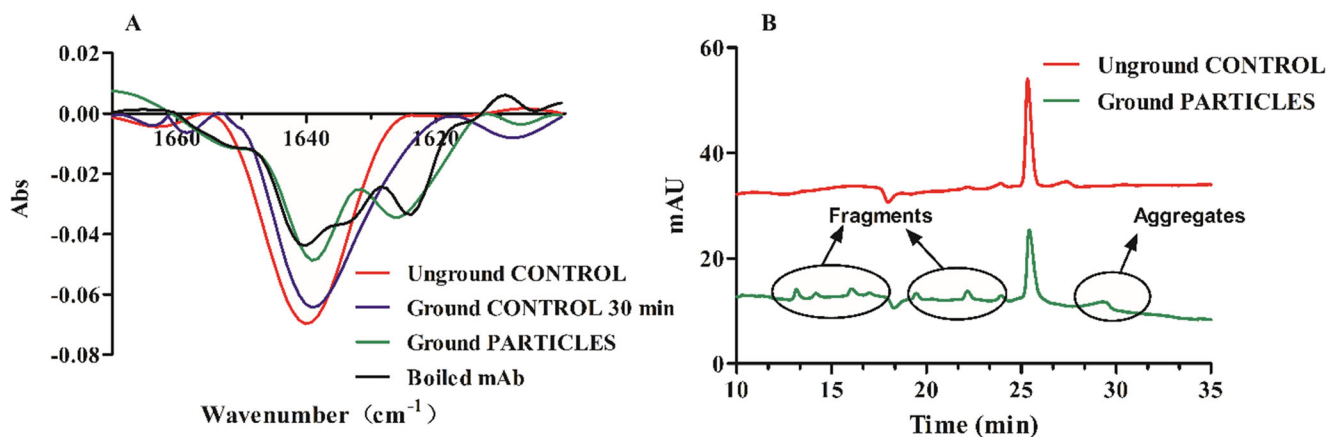


**Fig. 5** (A) Fourier transform infrared spectroscopy (second-order derivative) and (B) nonreduced CE-SDS of protein formulations without the scavenger.

With the research and development of biopharmaceutical tablets, more and more researchers have also considered the influence of mechanical stress such as grinding during tablet compression on the structure and activity of biopharmaceuticals. As early as 2002, there was a study suggesting that applying pressure to a solid powder would reduce the activity of different types of amylases (32). In 2015, another researcher studied the effect of tablet pressure on the conformation, temperature ( $T_m$ ) and folding reversibility after thermal denaturation of trypsin (33). Another group of researchers studied this process from a more mechanical point of view. Using bovine serum albumin (BSA) and lysozyme as model proteins, they

studied solid-state properties, mechanical properties, and compressibility, as well as the effect of tableting pressure, particle size and humidity on protein degradation (28). The research group recently published another study focusing on freeze-dried intravenous immunoglobulin (34). Two other studies conducted feasibility studies on an anti-tumor necrosis factor- $\alpha$  (TNF- $\alpha$ ) monoclonal antibody, infliximab tablets. The changes before and after granulation and tablet pressing were explored (27,35).

Although it is believed that the mechanical stress operation of grinding biological drugs may be less likely to be performed directly, its presence in the actual production cannot be ignored. A study recently investigated this process by examining freeze-dried mAb powders that are ground and can be used in highly concentrated nonaqueous protein suspensions for subcutaneous administration. It was discovered that during dry ball milling without cooling, numerous proteins are damaged and SbVPs are generated, compared to cryogenic ball milling, which maintains protein integrity effectively during the micronization process (36). As presented in this article, the temperature was high enough to generate freeze-dried particles during grinding at a local level (37,38). In addition to this known protein degradation due to the high temperature caused by mechanical grinding, a supplementary mechanism exists in which a certain mAb in a dry state can produce free radicals during mechanical grinding, resulting in the formation of SbVPs (16,39). However, since the effects of shearing and interfacial interactions on biopharmaceuticals have not been fully investigated, the stress sensitivity of each protein should be carefully considered (4). In this study, it is anticipated that another mAb-X exhibited similar results under grinding, with temperature and free radicals as the major causes of SbVP formation.

Some other methods used for mixing liquid formulations of mAb or recombinant freeze-dried formulations, such as stirring and shaking, have also been investigated (40,41). Stirring causes vial friction between the powder and the wall, which causes local heating and thus thermal stress, explaining the

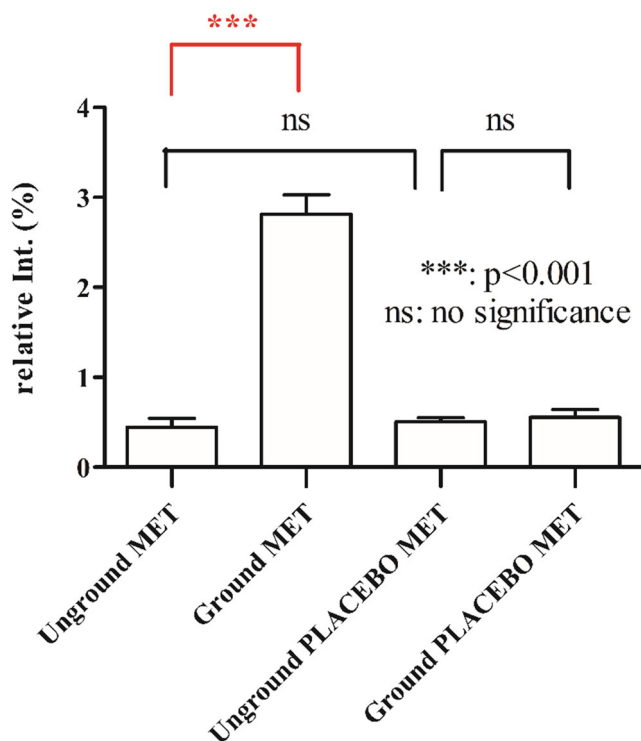


**Fig. 6** Relative total ion chromatogram intensity of Met(O) to Met in the unground and ground mAb-X MET and PLACEBO MET formulations as determined using liquid chromatography–mass spectrometry.



aggregation caused by stirring (13,42). SbVPs are formed during other processes of biopharmaceuticals, such as transportation and application as well. It has been reported that dropping can also cause protein degradation and aggregation in freeze-dried formulations, with the mechanism similar to that of temperature and free radical production (39). The same group also discussed the positive protective effect of secondary packaging on freeze-dried formulations (43), which was not detected in liquid formulations (44). In another study, a liquid formulation without polysorbate showed a significant increase in submicron and visible particles after the transfer, while there was minimal change in the presence of polysorbate (12).

As in a previous study on grinding (16), we proposed that lyophilized monoclonal antibody formulations subjected to mechanical stress (grinding) generate subvisible particles due to temperature and free radical generation. However, because of the complex nature of biological drugs, the stress sensitivity of each monoclonal antibody must be carefully examined. During the study of subvisible particles, some differences in the results of the various analytical methods were also discovered, and a gradient of grinding time was set up in this study to continue the investigation, and the advantages and disadvantages of each analytical method are also described below. The visible particles produced by increasing the grinding time were not explored in depth before, and in this study, their enrichment was followed by structural determination to reach reliable conclusions. Additionally, LC–MS was used to investigate the previously unexplored antioxidant mechanism of methionine.

Different analytical methods are commonly used to analyze aggregation and SbVPs (45). However, they have their advantages and disadvantages (46). Visual inspection is simple but the sensitivity is limited. According to the guidelines described in USP 788 (USP 41 Official Monograph for Particulate Matter in Injections, pp. 6537–6540, 2011), SbVP measurement specifies light obscuration as the preferred analysis method, however, the counting accuracy may not be satisfying because protein aggregates are mostly translucent and amorphous (47). Microscopes can provide a lot of information; however, it requires a lot of sample preparation time and its accuracy depends on the researcher.

MFI and FlowCam are two FIM methods that provide the advantages of manual microscopes while providing the additional advantages of instrument automation, high sensitivity, and low sample volume requirement (48,49). The detection sensitivity of these methods is higher than the light obscuration method for detecting micron-scale insoluble particles in the Chinese Pharmacopoeia (2015 edition), especially when detecting SbVPs with a small difference in refractive index from the environment. Therefore, they are currently used for screening and stability studies of mAb insoluble particles (50,51). FlowCam can record higher-quality particle images than MFI, which may better help identify the source of particles and thus characterize them (52,53).

SE-HPLC can maintain the natural conformation of proteins since it uses a gentle mobile phase and can characterize the ratio of dimers and oligomers at the nanoscale, as well as purity (5). One shortcoming is that the size range it can detect is limited to approximately 5–1000 kDa. Another limitation is that the loss of natural protein or increase in soluble aggregate levels can only be accurately quantified at a relatively high amount (i.e., more than 0.1% to 0.5% of the total protein) (54,55).

DLS is a simple and nondestructive technique for detecting high-molecular physical and chemical aggregates (5). Presently, it is widely used to measure particles with a size distribution ranging from 1 ~ 2 nm to 3 ~ 5  $\mu$ m. However, it also has the disadvantages of being unable to quantify particles, being unsuitable for polydisperse samples, and having low resolution. Besides, UV–Vis spectroscopy, flow field fractionation, nanoparticle tracking analysis, and analytical ultracentrifugation (AUC) can also be used as complementary techniques for particle analysis (56).

In this study, the SbVPs formed in the sample, which was detected using the FIM particle analysis method, did not affect the total peak area as measured by SE-HPLC. The area remains at approximately 100% despite some stress on the region. We observed a slight decrease in protein recovery only after grinding for 10 and 30 min. Therefore, SbVPs did not exhibit a substantial reduction in total protein content, which was validated by the results of the UV–Vis analysis. In this experiment, although SbVP levels significantly increased due to grinding for 30 s, SE-HPLC could not sensitively measure the aggregates produced in the mAb-X, i.e., the quality and purity of the monomer protein remained almost unchanged, and the second peak of DLS could hardly be detected. This was confirmed by the appropriate extension of the grinding time to 1, 10, and 30 min. FIM detected the significantly increased particles very sensitively, DLS detected a more obvious SbVP peak, while the peak area and purity of SE-HPLC remained unaltered. This difference can be explained by the fact that the FIM method is extremely sensitive, accounting for a small percentage of the total protein mass. The sensitivity of DLS is therefore between FIM and SE-HPLC in studying grinding-induced degradation of the freeze-dried mAb-X formulation. The sensitivity of the visual inspection method was slightly higher than that of SE-HPLC, while the UV–Vis results were aligned with that of SE-HPLC.

To investigate if SbVPs produced after grinding had undergone chemical modifications, we conducted several experiments on mAb-X, which was ground for a long time. After collecting the particles produced by grinding for 30 min, the secondary structure changed as measured by FT-IR. The intramolecular  $\beta$ -sheet structure is transformed into an intermolecular  $\beta$ -sheet structure, but the particles must be collected to detect structural changes. Otherwise, the results did not show an obvious change in secondary structure. Some covalent

aggregates and fragments appeared in the collected particles as measured by CE-SDS. A similar result was observed in another bubbling study of mAb samples, where no significant structural change was detected in the far-UV and near-UV circular dichroism (CD) spectra of the sample supernatant (57). In contrast, after the aggregates of their stress samples were prepared as dried pellets for IR detection, slight changes in the spectra were discovered, indicating possible changes in the secondary structure of the aggregated IgG (57). However, Psimadas et al. collected the particles produced during the freezing and thawing process and then used IR to detect their secondary structure, which showed little difference due to freezing and thawing (54). In this experiment, the changes in secondary structure and aggregates were detected by enriching the SbVPs produced by grinding stress. Compared with the spectra of native mAb-X, it revealed that the formed SbVPs lost a certain native structure. Proteins with structural changes have a strong tendency to aggregate. In the future, excipients that can maintain the native structure will be investigated for further mechanisms of aggregation caused by grinding stress, therefore thoroughly addressing the stability and aggregation issue.

The mechanism of Met oxidation in mAb formulations was also studied. Previous studies have discovered that free radical initiators, such as 2,2'-Azobis(2-amidinopropane) dihydrochloride, can induce aggregation by forming covalent bonds through free radical reaction (58). At high temperatures, 2,2'-Azobis(2-amidinopropane) dihydrochloride is thermally unstable and can generate alkyl radicals, peroxy radicals, and alkoxy radicals, which can effectively oxidize methionine, tryptophan, and other unstable residues in protein, and also cause additional physical and chemical degradation (59). This article discovered that grinding can produce free radicals and induce mAb-X aggregation as well. EPR results revealed that macromolecules produced free radicals during grinding, and Met acted as an antioxidant (18), which scavenged free radicals and protected mAb-X by generating Met(O). This also corresponds to LC-MS results. Based on existing data, no Met(O) was observed when grinding the small molecule excipients, indicating that only macromolecules produce free radicals during freeze-dried powder grinding.

## CONCLUSIONS

Conclusively, it has been shown that mAb-X can significantly produce SbVPs under mechanical stress of grinding, most likely due to high temperatures and generation of free radicals. The sensitivity of various particle analysis techniques in characterizing SbVPs has also been evaluated, with FIM being the most sensitive, followed by DLS, and SE-HPLC and UV-Vis being the least sensitive. Visual inspection has slightly higher sensitivity than SE-HPLC and UV-Vis. The

secondary structure of the particles produced after extended grinding was also characterized, indicating that the SbVPs formed have significantly different secondary structures than the native protein. The antioxidant mechanism of Met as a free radical scavenger was also investigated further. The result suggests that milder processing procedures and optimization of formulations, such as minimizing exposure to mechanical stress and addition of thermal stabilizers and free radical scavengers, should be used for the entire process from upstream production to individual administration of protein formulations, such as mAb, that tend to aggregate. Care should be taken to apply different validation methods during subsequent particle analysis to control immunogenic SbVPs.

## ACKNOWLEDGMENTS AND DISCLOSURES

We appreciate the National Natural Science Foundation of China (Grant No. 81741144) and the Ministry of Science and Technology of China (Grant No. 2018ZX09J18107-002) for their financial support. We also thank Ms. Xinyu Wang at Zhejiang University for performing the EPR experiments and Zhejiang Bioray Biopharmaceutical for providing us with mAb-X used for this study. Special thanks to Fluid Imaging Technologies for providing access to their FlowCam 8100. The authors declare that they have no known competing financial or personal interest conflict.

## REFERENCES

1. Strickley RG, Lambert WJ. A review of formulations of commercially available antibodies. *J Pharm Sci.* 2021;110:2590–608.
2. Pham NB, Meng WS. Protein aggregation and immunogenicity of biotherapeutics. *Int J Pharm.* 2020;585:119523.
3. Paul M, Astier A. Mechanically-induced aggregation of the monoclonal antibody cetuximab. *Ann Pharm Fr.* 2009;67:340–52.
4. Kiese S, Pappenberg A, Friess W, Mahler HC. Shaken, not stirred: mechanical stress testing of an IgG1 antibody. *J Pharm Sci.* 2008;97:4347–66.
5. Al-Ghobashy MA, Mostafa MM, Abed HS, Fathalla FA, Salem MY. Correlation between dynamic light scattering and size exclusion high performance liquid chromatography for monitoring the effect of pH on stability of biopharmaceuticals. *J Chromatogr B.* 2017;1060:1–9.
6. Das TK, Narhi LO, Sreedhara A, Menzen T, Grapentin C, Chou DK, Antochshuk V, Filipe V. Stress factors in mAb drug substance production processes: critical assessment of impact on product quality and control strategy. *J Pharm Sci.* 2020;109:116–33.
7. Gikanga B, Eisner DR, Ovadia R, Day ES, Stauch OB, Maa YF. Processing impact on monoclonal antibody drug products: protein subvisible particulate formation induced by grinding stress. *PDA J Pharm Sci Technol.* 2017;71:172–88.
8. Nayak A, Colandene J, Bradford V, Perkins M. Characterization of subvisible particle formation during the filling pump operation of a monoclonal antibody solution. *J Pharm Sci.* 2011;100:4198–204.
9. Duerkop M, Berger E, Dürauer A, Jungbauer A. Influence of cavitation and high shear stress on HSA aggregation behavior. *Eng Life Sci.* 2017;00:1–10.

10. Telikepalli SN, Kumru OS, Kalonia C, Esfandiary R, Joshi SB, Middaugh CR, Volklin DB. Structural characterization of IgG1 mAb aggregates and particles generated under various stress conditions. *J Pharm Sci.* 2014;103:796–809.
11. Tyagi AK, Randolph TW, Dong A, Maloney KM, Hitscherich C, Carpenter JF. IgG particle formation during filling pump operation: a case study of heterogeneous nucleation on stainless steel nanoparticles. *J Pharm Sci.* 2009;98:94–104.
12. Siska C, Harber P, Kerwin BA. Shocking data on parcel shipments of protein solutions. *J Pharm Sci.* 2020;109:690–5.
13. Telikepalli S, Kumru OS, Kim JAEH, Joshi SB, Berry KBO, Blake-haskins AW, et al. Characterization of the physical stability of a lyophilized IgG1 mAb after accelerated shipping-like stress. *Pharm Biotechnol.* 2015;104:495–507.
14. Singh SN, Kumar S, Bondar V, Wang N, Forcino R, Colandene J, Nesta D. Unexplored benefits of controlled ice nucleation: lyophilization of a highly concentrated monoclonal antibody solution. *Int J Pharm.* 2018;552:171–9.
15. Wang H, Zheng H, Wang Z, Bai H, Carpenter JF, Chen S, et al. Formation of protein sub-visible particles during vacuum degassing of etanercept solutions. *Int J Biol Macromol.* 2014;66:151–7.
16. Qian C, Wang G, Wang X, Barnard J, Gao J, Bao W. Formation of protein sub-visible particles during powder grinding of a monoclonal antibody. *Eur J Pharm Biopharm.* 2020;149:1–11.
17. Hawkins CL, Davies MJ. Generation and propagation of radical reactions on proteins. *Biochim Biophys Acta.* 2001;1504:196–219.
18. Dion MZ, Leiske D, Sharma VK, Zafra CLZ De, Salisbury CM. Mitigation of oxidation in therapeutic antibody formulations : A biochemical efficacy and safety evaluation of N -acetyl-tryptophan and L-methionine. *Pharm Res* 2018;35:222.
19. Bommana R, Mozziconacci O, John Wang Y, Schöneich C. An efficient and rapid method to monitor the oxidative degradation of protein pharmaceuticals: probing tyrosine oxidation with fluorogenic derivatization. *Pharm Res.* 2017;34:1428–43.
20. Vass P, Hirsch E, Kóczyán R, Démuth B, Farkas A, Fehér C, Szabó E, Németh Á, Andersen SK, Vigh T, Verreck G, Csontos I, Marosi G, Nagy ZK. Scaled-up production and tableting of grindable electrospun fibers containing a protein-type drug. *Pharmaceutics.* 2019;11:1–12.
21. Vass P, Nagy ZK, Kóczyán R, Fehér C, Démuth B, Szabó E, Andersen SK, Vigh T, Verreck G, Csontos I, Marosi G, Hirsch E. Continuous drying of a protein-type drug using scaled-up fiber formation with HP- $\beta$ -CD matrix resulting in a directly compressible powder for tableting. *Eur J Pharm Sci.* 2020;141:105089.
22. Lee PW, Maia J, Pokorski JK. Milling solid proteins to enhance activity after melt-encapsulation. *Int J Pharm.* 2018;533:254–65.
23. Ettl EE, Winter G, Engert J. Toward intradermal vaccination: preparation of powder formulations by collapse freeze-drying. *Pharm Dev Technol.* 2014;19:213–22.
24. Anamur C, Winter G, Engert J. Stability of collapse lyophilized influenza vaccine formulations. *Int J Pharm.* 2015;483:131–41.
25. Tantisirpreecha C, Jaturanpinyo M, Panyarachun B, Sarisuta N. Development of delayed-release proliposomes tablets for oral protein drug delivery. *Drug Dev Ind Pharm.* 2012;38:718–27.
26. Wong CY, Martínez J, Carnagarin R, Dass CR. In-vitro evaluation of enteric coated insulin tablets containing absorption enhancer and enzyme inhibitor. *J Pharm Pharmacol.* 2017;69:285–94.
27. Maurer JM, Hofman S, Schellekens RCA, Tonnis WF, Dubois AOT, Woerdenbag HJ, Hinrichs WLJ, Kosterink JGW, Frijlink HW. Development and potential application of an oral ColoPulse infliximab tablet with colon specific release: a feasibility study. *Int J Pharm.* 2016;505:175–86.
28. Wei Y, Wang C, Jiang B, Sun CC, Middaugh CR. Developing biologics tablets: the effects of compression on the structure and stability of bovine serum albumin and lysozyme. *Mol Pharm.* 2019;16:1119–31.
29. Farinha S, Moura C, Afonso MD, Henriques J. Production of lysozyme-PLGA-loaded microparticles for controlled release using hot-melt extrusion. *AAPS PharmSciTech.* 2020;21:1–14.
30. Rajkhowa R, Hu X, Tsuzuki T, Kaplan DL, Wang X. Structure and biodegradation mechanism of milled Bombyx mori silk particles. *Biomacromolecules.* 2012;13:2503–12.
31. Kazemimostaghim M, Rajkhowa R, Patil K, Tsuzuki T, Wang X. Structure and characteristics of milled silk particles. *Powder Technol.* 2014;254:488–93.
32. Picker KM. Influence of tableting on the enzymatic activity of different  $\alpha$ -amylases using various excipients. *Eur J Pharm Biopharm.* 2002;53:181–5.
33. Klukkert M, Weert MVANDE, Fanø M, Rades T, Leopold CS. Influence of tableting on the conformation and thermal stability of trypsin as a model protein. *J Pharm Sci.* 2015;104:4314–21.
34. Lu Y, Wang C, Jiang B, Sun CC, Ph D, Hoag W, et al. Effects of compaction and storage conditions on stability of intravenous immunoglobulin – implication on developing oral tablets of biologics. *Int J Pharm.* 2021;604:120737.
35. Gareb B, Posthumus S, Beugeling M, Koopmans P, Touw DJ, Dijkstra G, Kosterink JGW, Frijlink HW. Towards the oral treatment of ileo-colonic inflammatory bowel disease with infliximab tablets: development and validation of the production process. *Pharmaceutics.* 2019;11:428.
36. Marschall C, Graf G, Witt M, Hauptmeier B, Friess W. Preparation of high concentration protein powder suspensions by milling of lyophilizates. *Eur J Pharm Biopharm.* 2021;166:75–86.
37. Le Gall M, Guéguen J, Séve B, Quillien L. Effects of grinding and thermal treatments on hydrolysis susceptibility of pea proteins (*Pisum sativum* L.). *J Agric Food Chem.* 2005;53:3057–64.
38. Gikanga B, Hui A, Maa YF. Mechanistic investigation on grinding-induced subvisible particle formation during mixing and filling of monoclonal antibody formulations. *PDA J Pharm Sci Technol.* 2018;72:117–33.
39. Fang W, Liu J, Zheng H, Shen B. Protein sub-visible particle and free radical formation of a freeze-dried monoclonal antibody formulation during dropping. *J Pharm Sci.* 2021;110:1625–34.
40. Koepf E, Eisele S, Schroeder R, Brezesinski G, Friess W. Notorious but not understood: how liquid-air interfacial stress triggers protein aggregation. *Int J Pharm.* 2018;537:202–12.
41. Koepf E, Schroeder R, Brezesinski G, Friess W. The film tells the story: physical-chemical characteristics of IgG at the liquid-air interface. *Eur J Pharm Biopharm.* 2017;119:396–407.
42. Gikanga B, Chen Y, Stauch OB, Maa YF. Mixing monoclonal antibody formulations using bottom-mounted mixers: impact of mechanism and design on drug product quality. *PDA J Pharm Sci Technol.* 2015;69:284–96.
43. Fang WJ, Liu JW, Barnard J, Wang H, Qian YC, Xu J. Effects of secondary package on freeze-dried biopharmaceutical formulation stability during dropping. *J Pharm Sci.* 2021;110:2916–24.
44. Fang WJ, Liu JW, Gao H, Qian YC, Gao JQ, Wang H. Secondary packages cannot protect liquid biopharmaceutical formulations from dropping-induced degradation. *Pharm Res.* 2021;38:1397–404.
45. Yoneda S, Niederleitner B, Wiggenhorn M, Koga H, Totoki S, Krayukhina E, Friess W, Uchiyama S. Quantitative laser diffraction for quantification of protein aggregates: comparison with resonant mass measurement, nanoparticle tracking analysis, flow imaging, and light obscuration. *J Pharm Sci.* 2019;108:755–62.
46. Zöls S, Weinbuch D, Wiggenhorn M, Winter G, Friess W, Jiskoot W, Hawe A. Flow imaging microscopy for protein particle analysis — a comparative evaluation of four different analytical instruments. *Am Assoc Pharm Sci.* 2013;15:1200–11.
47. Huang C, Sharma D, Oma P, Krishnamurthy R. Quantitation of protein particles in parenteral solutions using micro-flow imaging. *J Pharm Sci.* 2009;98:3058–71.

48. Werk T, Volkin DB, Mahler H. Effect of solution properties on the counting and sizing of subvisible particle standards as measured by light obscuration and digital imaging methods. *Eur J Pharm Sci.* 2014;53:95–108.
49. Wilson GA, Manning MC. Flow imaging : moving toward best practices for subvisible particle quantitation in protein products. *J Pharm Sci.* 2013;102:1133–4.
50. Vollrath I, Mathaes R, Sediq AS, Jere D, Jörg S, Huwyler J, Mahler HC. Subvisible particulate contamination in cell therapy products—can we distinguish? *J Pharm Sci.* 2020;109:216–9.
51. Weinbuch D, Zöls S, Wiggenhorn M, Friess W, Winter G, Jiskoot WHA. Micro–flow imaging and resonant mass measurement (archimedes)—complementary methods to quantitatively differentiate protein particles and silicone oil droplets. *J Pharm Sci.* 2013;102:2152–65.
52. Kiyoshi M, Shibata H, Harazono A, Torisu T, Maruno T, Akimaru M, Asano Y, Hirokawa M, Ikemoto K, Itakura Y, Iwura T, Kikitsu A, Kumagai T, Mori N, Murase H, Nishimura H, Oda A, Ogawa T, Ojima T, et al. Collaborative study for analysis of subvisible particles using flow imaging and light obscuration : experiences in Japanese biopharmaceutical consortium. *J Pharm Sci.* 2018;108:332–41.
53. Mathaes R, Manning MC, Winter G, Engert J, Wilson GA. Shape characterization of subvisible particles using dynamic imaging analysis. *J Pharm Sci.* 2020;109:375–9.
54. Psimadas D, Georgoulas P, Valotassiou V, Loudos G. Subvisible particle counting provides a sensitive method of detecting and quantifying aggregation of monoclonal antibody caused by freeze-thawing: insights into the roles of particles in the protein aggregation pathway. *J Pharm Sci.* 2012;101:2271–80.
55. Den Engelsman J, Garidel P, Smulders R, Koll H, Smith B, Bassarab S, et al. Strategies for the assessment of protein aggregates in pharmaceutical biotech product development. *Pharm Res.* 2011;28:920–33.
56. Wolfrum S, Weichsel U, Siedler M, Weber C, Peukert W. Monitoring of flow-induced aggregation and conformational change of monoclonal antibodies. *Chemie Ing Tech.* 2017;89:987–94.
57. Sreenivasan S, Jiskoot W, Rathore AS. Rapid aggregation of therapeutic monoclonal antibodies by bubbling induced air/liquid interfacial and agitation stress at different conditions. *Eur J Pharm Biopharm.* 2021;168:97–109.
58. Ji JA, Zhang B, Cheng W, Wang YJ. Methionine, tryptophan, and histidine oxidation in a model protein, PTH: mechanisms and stabilization. *J Pharm Sci.* 2009;98:4485–500.
59. Zheng K, Ren D, Wang YJ, Lilyestrom W, Scherer T, Hong JKY, Ji JA. Monoclonal antibody aggregation associated with free radical induced oxidation. *Int J Mol Sci.* 2021;22:3952.

**Publisher's Note** Springer Nature remains neutral with regard to jurisdictional claims in published maps and institutional affiliations.